


# Continuous Symmetry Measure vs Voronoi Entropy of Droplet Clusters

Mark Frenkel, Alexander A. Fedorets, Leonid A. Dombrovsky, Michael Nosonovsky, Irina Legchenkova, and Edward Bormashenko\*

 Cite This: *J. Phys. Chem. C* 2021, 125, 2431–2436

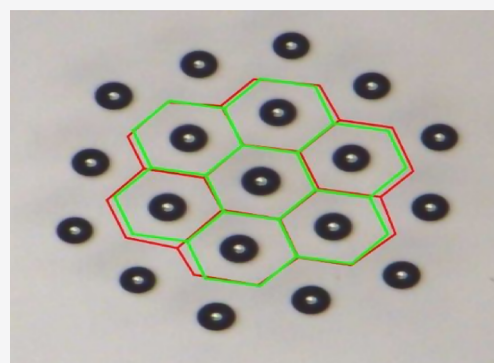
 Read Online

ACCESS |

 Metrics & More

 Article Recommendations

**ABSTRACT:** Symmetry and orderliness of two-dimensional (2D) levitating microdroplet clusters are quantified with the Voronoi entropy (VE) and the continuous symmetry measure (CSM). The time evolution of both VE and CSM is investigated. To compare the correlation between the two measures of orderliness, the Pearson correlation coefficient (PCC) was calculated. The maximum correlation between the VE and CSM was found for clusters containing the number of droplets enabling the formation of hexagons, i.e., droplet clusters possessing 6-fold symmetry. In other cases, the maxima and minima of the VE and CSM are not always well correlated; moreover, in certain cases, maxima of the CSM may correspond to the minima of the VE. Symmetry and orderliness of 2D patterns could not be quantified with a single mathematical measure.



## 1. INTRODUCTION

The concept of symmetry arises from Greek *συμμετρία* (symmetria), which means an agreement in dimensions due to proportion or by arrangement.<sup>1</sup> In classical antiquity, symmetry meant commensurability and it was believed to constitute a canon of beauty in nature and in art.<sup>1</sup> In mathematics, “symmetry” implies an invariance of an object subjected to certain transformations, such as translations, reflections, rotations, or scaling.<sup>2</sup> Symmetry considerations play a fundamental role in modern physics and chemistry,<sup>2–6</sup> leading to the laws of conservation in physics<sup>7</sup> and being dominant in the particle physics,<sup>8</sup> field theory,<sup>8</sup> quantum theory,<sup>9,10</sup> crystallography,<sup>11</sup> condensed-matter physics,<sup>12</sup> thermodynamics,<sup>13,14</sup> chemistry, and biology.<sup>1–5</sup> Moreover, symmetry considerations are of fundamental importance in aesthetics and in science–art relations.<sup>1,15</sup>

It is usually implied that symmetry changes abruptly or intermittently. In other words, symmetry is viewed as a binary feature, when an object is considered as either symmetric or asymmetric. Despite this, a fundamentally new approach to quantifying symmetry as a continuous measure of a pattern, such as a two-dimensional (2D) set of points, was suggested and tested recently by Zabrodsky and co-workers.<sup>16–20</sup> They introduced a continuous measure of deviation from the symmetry of shapes, defined as the sum of minimum squared distances required to move the points of the original shape to obtain a symmetrical shape. The suggested continuous symmetry measure (CSM) is applicable to various types of symmetries in any dimensions.<sup>16–20</sup> Such an approach to

symmetry broke the “black–white” paradigm usually adopted for the analysis of the symmetry of patterns.

We implement this approach for the analysis of the symmetry of 2D droplet clusters levitating above heated water/vapor interfaces.<sup>21–23</sup> It was demonstrated by our group earlier that such self-assembled 2D clusters of monodispersed condensed water microdroplets could levitate over a locally heated layer of water, as depicted in Figure 1.<sup>21–23</sup> Large clusters form hexagonally ordered (honeycomb) structures similar to colloidal crystals, while small (from one to several dozens of droplets) clusters possess special symmetry properties. Small clusters, in particular, may demonstrate 4-fold, 5-fold, and 7-fold symmetry, which is absent from large clusters and crystals. The symmetry properties of small cluster configurations are universal, i.e., they do not depend on the size of droplets and details of the interactions between them.<sup>24,25</sup> We demonstrated that various approaches enabling quantification and monitoring time evolution of the symmetry of droplet clusters are possible, including the Voronoi entropy (VE)<sup>26,27</sup> and ADE classification.<sup>28</sup>

In the present paper, we quantified the symmetry of droplet clusters with the continuous symmetry measure (CSM)<sup>16–26</sup>

**Received:** November 18, 2020

**Revised:** January 10, 2021

**Published:** January 25, 2021



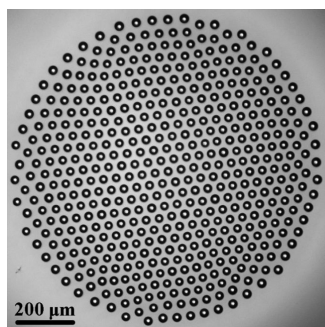


**Figure 1.** Typical droplet cluster levitating above the water surface. Scale bar is 200  $\mu\text{m}$ .

in parallel with the calculation of the appropriate Voronoi entropy.<sup>26,27,29</sup> The Voronoi tessellation of the diagram of a 2D area with a set of nodes in it divides the area into polygonal zones or cells, with each cell containing points that are closest to a given node. Such tessellation represents the 2D special case of the Wigner–Seitz cell tessellation.<sup>30</sup> We calculate the CSM of a Voronoi diagram of a droplet cluster and not the CSM of the cluster itself, considering the theorem stating that a Voronoi cell always has the same point symmetry group as the underlying lattice of the 2D pattern.<sup>30</sup>

Large levitating droplet clusters demonstrate 6-fold symmetry, as shown in Figure 1, and in accordance with the Neuman–Minnigerode–Curie principle, their physical properties (such as planar density, thermal, and electrical conductivity) must be invariant with respect to the symmetry group of hexagon.<sup>31</sup>

## 2. METHODS

Levitating droplet clusters were generated according to the protocol described in detail earlier.<sup>22–25</sup> Experiments were carried out with distilled water containing microconcentration of surfactants suppressing the thermocapillary flows, as described in ref 32. The experimental setup included a cuvette with a submillimeter-thick layer of water, heated from the bottom by an Omicron Laserage BrixX 808-800HP semiconductor laser, wavelength 0.808  $\mu\text{m}$ . The unit including a peristaltic pump and a confocal distance sensor provided the control thickness of the water layer within  $200 \pm 1 \mu\text{m}$ . The water temperature at the periphery of the water layer was kept at the level of  $3.8 \pm 0.3 \text{ }^\circ\text{C}$ .

The laser beam was focused on the spot with a diameter of 1 mm. The temperature field at the water/vapor interface was registered with a FLIR A65Sc thermocamera (spectral range, 7.5–14.0  $\mu\text{m}$ ; thermal resolution,  $\Delta T = 0.05 \text{ K}$ ). The thermal camera was equipped with macro-objective close-up IR 2.9 $\times$  (the dimension of the pixel within the infrared (IR) image was 0.05 mm). The control of laser beam power was performed with the Thorlabs units, namely, the PM200 control block and the S401C power sensor (spectral range, 0.19–10.6  $\mu\text{m}$ ; power range, 10  $\mu\text{W}$  to 1 W; accuracy,  $\pm 5\%$ ). Videos were taken with a Zeiss Axio Zoom V16 microscope, equipped with a pco.edge 5.5 charge-coupled device (CCD) camera.

The generation of clusters built of the constant number of droplets was carried out in two stages. In the first stage, the power of the laser was fixed at a low level, providing the maximal local temperature of 37  $^\circ\text{C}$ . At this stage, droplets easily entered the heated gas area. When the desired number of droplets was attained, the power of the laser was abruptly

increased, providing the temperature of the heated water spot of 67  $^\circ\text{C}$ . Heating yielded the consequent increase in the velocity of the steam–air flow. Condensing droplets, which entered into the heated spot were heavy enough for levitation, whereas new-born small droplets were blown out by the ascending steam–air flow. Thus, the resulting stable droplet cluster, such as depicted in Figure 1, built of the fixed number of droplets of almost equal diameters was created.

## 3. RESULTS AND DISCUSSION

Let us define the continuous symmetry measure (CSM). Consider a nonsymmetrical shape built of  $n_k$  points  $M_i$  ( $i = 1, 2, \dots, n_k$ ) and a given symmetry group  $G$ . The CSM, denoted as  $S(G)$ , is a function of the minimal average square displacement the points  $M_i$  of the shape have to undergo to acquire the prescribed  $G$  symmetry. Assume that the  $G$ -symmetrical shape emerges from the set of points  $\hat{M}_i$ . Since the set  $\hat{M}_i$  is established, the continuous symmetry measure is defined as

$$S(G) = \frac{1}{n_p} \sum_{i=1}^{n_p} |M_i - \hat{M}_i|^2 \quad (1)$$

(square values in eq 1 are taken so that the function is isotropic, continuous, and differentiable). First, the points of the nearest shape possessing the  $G$  symmetry should be identified. The algorithm enabling identification of the set of points  $\hat{M}_i$  constituting this symmetrical shape is suggested in refs 16–20. The example supplied in Figure 2 depicts an

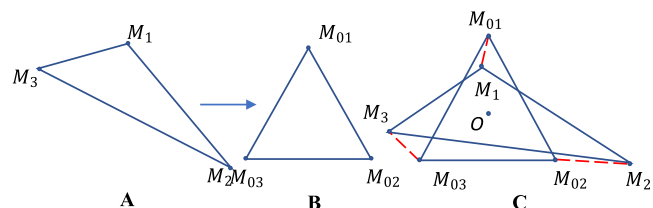


**Figure 2.** Calculation of the CSM for the triangle  $M_1M_2M_3$  (A). (B) Equilateral triangle  $M_{01}M_{02}M_{03}$  represents the symmetrical shape corresponding to the given triangle  $M_1M_2M_3$ . (C) Calculation of CSM. Point  $O$  is the common centroid.

equilateral triangle  $M_{01}M_{02}M_{03}$  representing the symmetric shape corresponding to the given triangle  $M_1M_2M_3$ . The symmetric equilateral triangle  $M_{01}M_{02}M_{03}$  emerges from the transformation of the given triangle  $M_1M_2M_3$  as follows: vertex  $M_i$  is rotated counterclockwise around the centroid  $O$  of the pristine triangle  $M_1M_2M_3$  by  $\frac{2\pi(i-1)}{3}$  radians (in other words, one of vertices of the triangle  $M_1M_2M_3$  remains fixed); thus, the triangle  $M_1M_2M'_3$  emerges. Afterward, the location of the centroid  $O'$  of the triangle  $M_1M_2M'_3$  is identified. Centroid  $O'$  is rotated clockwise around the centroid  $O$  by  $-\frac{2\pi(i-1)}{3}$  radians. Thus, the equilateral triangle  $M_{01}M_{02}M_{03}$  shown in Figure 2, representing the symmetrical shape closest to the pristine nonsymmetrical triangle  $M_1M_2M_3$ , is created.<sup>16–19</sup> Since the set  $\hat{M}_i$  is established, the CSM is calculated by eq 1. Consider that we calculate the CSM of the Voronoi diagram of the droplet cluster and not of the cluster itself. The point symmetry group of the polygonal Voronoi cells coincides with the symmetry group of the pristine droplet cluster.<sup>30</sup>

As suggested in refs 16–20, CSM introduced by eq 1 estimates a “minimal effort” necessary for the transformation of

an original shape into the symmetric one. The idea of such a minimal effort resembles the Gauss principle of least constraint, which is equivalent to the Hamilton's variational principle in classical mechanics.<sup>33</sup> Minimization of CSM and the Gauss principle of least constraint represent the least-squares principles.<sup>16–20,33</sup> The extremal (minimal) properties of the aforementioned procedure enabling minimization of CSM still require rigorous proof. Despite this, in our treatment of the symmetry of droplet clusters, we follow the procedure introduced in refs 16–19, which was successfully employed for the quantification of the symmetry of organic molecules.<sup>34–36</sup>

CSM of the triangle  $M_1M_2M_3$  corresponds to the sum  $S(G)$  introduced by eq 1. This is necessary for the transformation of the triangle  $M_1M_2M_3$  into the symmetrical one  $M_{01}M_{02}M_{03}$  (the symmetry group  $D_3$ ). The entire procedure of the calculation of the CSM is illustrated in Figure 2. Obviously, CSM, in this case, is given by eq 2

$$\text{CSM} = \frac{1}{3}(|M_1M_{01}|^2 + |M_2M_{02}|^2 + |M_3M_{03}|^2) \quad (2)$$

The details of the mathematical procedure enabling the calculation of CSM are supplied in refs 16–20. We applied the ideas suggested in refs 16–20 for the calculation of the time-dependent CSM for the droplet clusters, such as depicted in Figure 1, with one difference: the CSM was normalized to the distance between the initial and eventual centroids.

We calculated the CSM of the Voronoi diagrams emerging from the locations of centers of droplets in the cluster. The Voronoi diagram of a given cluster is composed of  $N$  polygons. The CSM was calculated for each polygon, as discussed above, and averaged. Thus, the time evolution of the averaged CSM of the cluster was elucidated. In parallel, the time evolution of the Voronoi entropy was calculated for the same droplet cluster. The Voronoi entropy of the given set of points corresponding to the Voronoi tessellation or diagram quantifies ordering in this set.<sup>26–29</sup> A Voronoi tessellation of an infinite plane is a partitioning of the plane into regions based on the distance to a specified discrete set of points (called seeds or nuclei<sup>26–29</sup>). For each seed, there is a corresponding region consisting of all points closer to that seed than to any other.<sup>26–29</sup> A typical Voronoi diagram corresponding to the real levitating droplet cluster is depicted in Figure 3. It is noteworthy that the Bond number for the droplets constituting the cluster is much smaller than unity; thus, all droplets may be represented by the points located in the centers of droplets.

The Voronoi entropy of the given set of points located in a plane is defined as

$$S_{\text{vor}} = - \sum_i P_i \ln P_i \quad (3)$$

where  $p_i$  is the fraction of polygons possessing  $n$  edges for a given Voronoi diagram (also called the coordination number of the polygon) and  $i$  is the total number of polygon types with different numbers of edges.<sup>26–29</sup> The summation in eq 3 is performed from  $i = 3$  to the largest coordination number of any available polygon, e.g., to  $i = 6$ , if a polygon with the largest number of edges is a hexagon.

Figure 4 depicts the time evolution of the averaged CSM and Voronoi entropy for a levitating droplet cluster built of 11 droplets. It is expected that the CSM and Voronoi entropy of the same cluster are correlated; indeed, both of these values quantify orderliness of the given 2D pattern. However, the situation is more complicated. Separated peaks in the CSM,

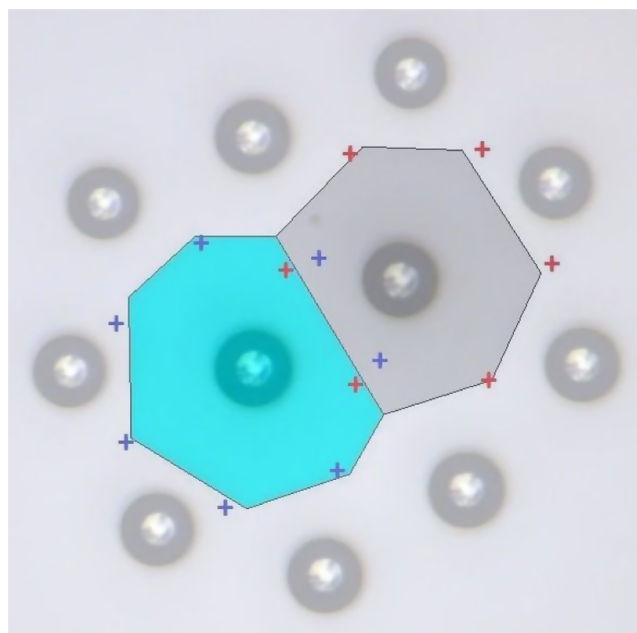


**Figure 3.** Voronoi diagram corresponding to the real droplet cluster. Vertices of the ideal polygons are depicted with crosses.

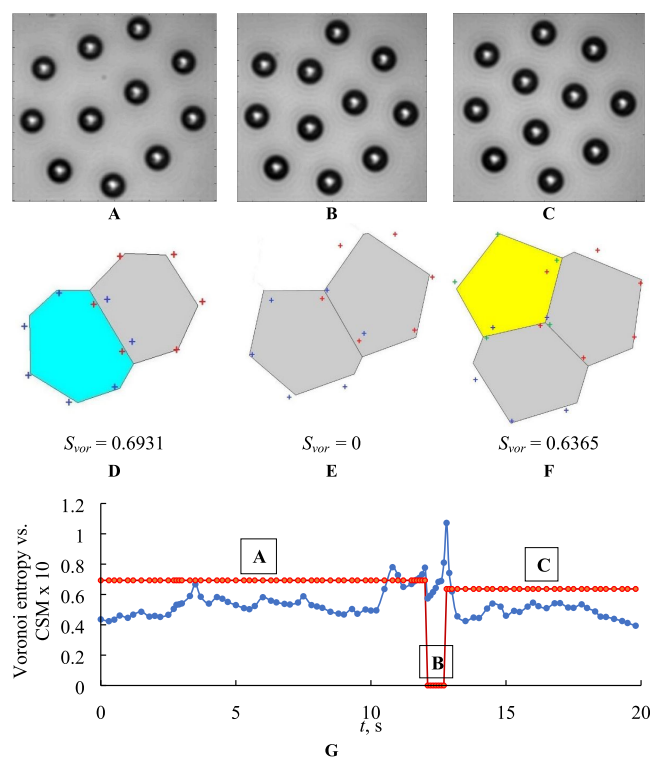


**Figure 4.** (A–C) Evolution of the levitating droplet cluster of 11 droplets. (D–F) Corresponding Voronoi diagrams and VE. Vertices of the ideal polygons are depicted with crosses. (G) Time dependences of the CSM and Voronoi entropy of the cluster are presented. The blue curve corresponds to the time evolution of Voronoi entropy and the red curve corresponds to the time dependence of CSM. Letters A, B, and C in black frames mark areas corresponding to the Voronoi entropy of D, E, and F tessellations.

recognized from Figure 4, correspond to the same value of the Voronoi entropy. Figure 5 depicting the time evolution of the

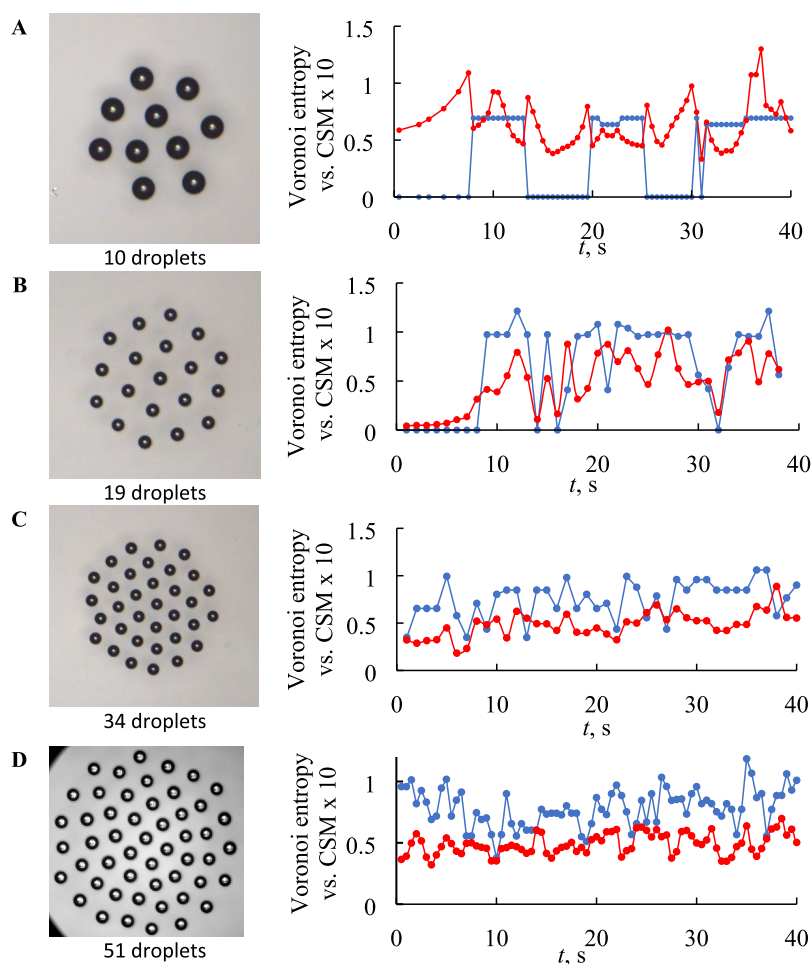


**Figure 5.** Time evolution of the CSM and Voronoi entropy for various levitating droplet clusters. The blue curve corresponds to the time evolution of Voronoi entropy and the red curve corresponds to the time dependence of CSM. The clusters contain: (A) 10 droplets;  $r_{xy} = 0.179$ ; (B) 19 droplets,  $r_{xy} = 0.747$ ; (C) 34 droplets,  $r_{xy} = 0.375$ ; and (D) 51 droplets;  $r_{xy} = 0.29$ .

CSM and Voronoi entropy for the droplet clusters built of 10, 19, 34, and 51 droplets supports this observation. Maxima and minima of the CSM and Voronoi entropy are not always correlated; moreover, maxima of CSM may correspond in time to the minima of the Voronoi entropy. What is the physical reason of the oscillations of the Voronoi entropy and CSM, recognized in Figure 5? It seems plausible to relate these oscillations to the vibrations of water droplets.<sup>37</sup> The characteristic frequencies of these vibrations are located in the range of  $f \cong 1\text{--}50$  Hz.<sup>37</sup>

It was instructive to estimate the correlation between the Voronoi entropy and CSM with the Pearson product-moment correlation coefficient  $r_{xy}$

$$r_{xy} = \frac{\sum (x - \bar{x})(y - \bar{y})}{\sqrt{\sum (x - \bar{x})^2 \sum (y - \bar{y})^2}} \quad (4)$$

where  $x$  and  $y$  are the values of the Voronoi entropy  $S_{\text{vor}}$  and CSM, respectively, and  $\bar{x}$  and  $\bar{y}$  are their averaged values using the frame-by-frame averaging of the cluster images. The values of the Pearson correlation coefficients  $r_{xy}$  are summarized in the caption of Figure 5. It is recognized that the maximal correlation between the Voronoi entropy and CSM ( $r_{xy} = 0.747$ ) is attained for the droplet cluster containing 19 droplets. It is seen that the cluster of 19 droplets enables construction possessing 6-fold symmetry, as shown in Figure

5B, whereas 10, 34, and 51 droplets do not allow the formation of completely symmetrical 6-fold patterns, and consequently, the correlation between the Voronoi entropy and the continuous measure of symmetry is low.

This observation is consistent with the hypothesis that orderliness and symmetry are strongly correlated in physical systems.<sup>13</sup> 2D levitating droplet clusters supply a flexible controlled model system enabling verification and quantification of this hypothesis. We recognize that the continuous measure of symmetry and the Voronoi entropy of the same pattern may be weakly correlated; this possibility is illustrated in Figure 6. The Voronoi tessellation presented in Figure 6 is built from the deformed identical hexagons. Obviously, the Voronoi entropy of such a tessellation is zero ( $S_{\text{vor}} = 0$ ); whereas, the CSM of the same pattern is not zero (CSM = 0.084) and this is due to the fact the presented hexagons are “distorted” from the ideal 6-fold symmetric shapes. Additional insights clarifying the interplay between the Voronoi entropy and CSM are necessary. However, it may be concluded that orderliness of 2D patterns could hardly be quantified with a single mathematical measure.

#### 4. CONCLUSIONS

We report quantifying of ordering in 2D patterns emerging from the droplet clusters levitating above the hot water. Well-

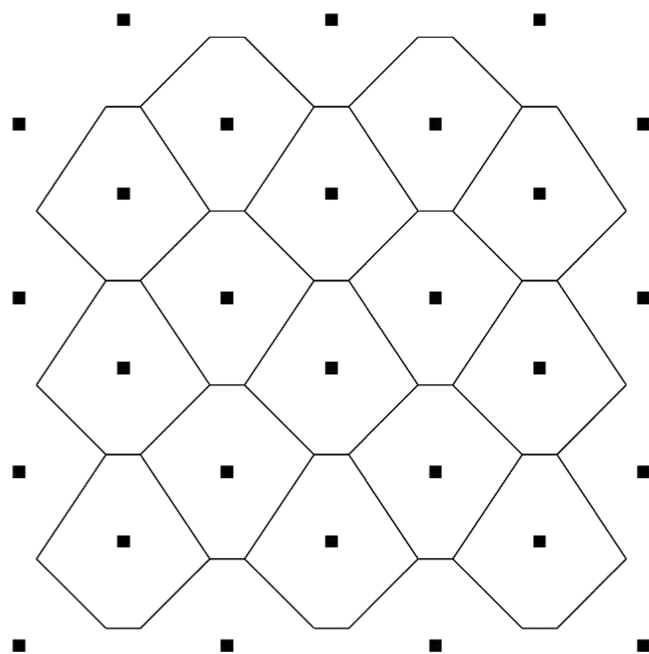


**Figure 6.** Voronoi tessellation built only of hexagons. The Voronoi entropy of the tessellation  $S_{\text{vor}} = 0$ , whereas  $\text{CSM} = 0.084$ .

ordered microdroplet clusters supply the fascinating laboratory system, enabling the model study of physical and biological processes.<sup>21–25,38,39</sup> We tested the hypothesis that ordering and symmetry in the droplet clusters are necessarily correlated.<sup>13</sup> It is usually assumed that the symmetry of physical objects or patterns changes intermittently; in other words, an object is considered as either symmetric or asymmetric. The alternative approach was suggested, developed, and tested in refs 16–20, in which symmetry was quantified with a continuous measure of the pattern. The authors of refs 16–20 suggested a continuous measure of symmetry, defined as the sum of the minimum squared distances required to move the points of the original pattern to obtain a symmetrical shape.<sup>16–20</sup> It was demonstrated that this continuous measure is applicable to any type of symmetry in any dimensions.<sup>16–20</sup> We compared the time evolution of the Voronoi entropy and the continuous measure of symmetry established in parallel for the same patterns emerging from water droplets forming the levitating clusters. The maximal Pearson correlation between the Voronoi entropy and continuous measure of symmetry was registered for the cluster built of 19 droplets, enabling the construction of the 2D pattern demonstrating the exact 6-fold symmetry. The relatively low Pearson correlation coefficient was inherent for clusters in which perfect symmetry was impossible. Thus, the Voronoi entropy and the continuous measure of symmetry, both quantifying ordering in 2D patterns, are not necessarily correlated. Thus, it seems plausible to suggest that orderliness of 2D point patterns could hardly be quantified with a single mathematical measure.

## AUTHOR INFORMATION

### Corresponding Author

**Edward Bormashenko** – Department of Chemical Engineering, Ariel University, Ariel 407000, Israel; [orcid.org/0000-0003-1356-2486](https://orcid.org/0000-0003-1356-2486); Email: [edward@ariel.ac.il](mailto:edward@ariel.ac.il)

## Authors

**Mark Frenkel** – Department of Chemical Engineering, Ariel University, Ariel 407000, Israel

**Alexander A. Fedorets** – Institute of Environmental and Agricultural Biology (X-BIO Institute), University of Tyumen, Tyumen 625003, Russia; [orcid.org/0000-0001-6595-3927](https://orcid.org/0000-0001-6595-3927)

**Leonid A. Dombrovsky** – Institute of Environmental and Agricultural Biology (X-BIO Institute), University of Tyumen, Tyumen 625003, Russia; Heat Transfer Department, Joint Institute for High Temperatures, Moscow 111116, Russia

**Michael Nosonovsky** – Institute of Environmental and Agricultural Biology (X-BIO Institute), University of Tyumen, Tyumen 625003, Russia; Department of Mechanical Engineering, University of Wisconsin–Milwaukee, Milwaukee, Wisconsin 53211, United States; [orcid.org/0000-0003-0980-3670](https://orcid.org/0000-0003-0980-3670)

**Irina Legchenkova** – Department of Chemical Engineering, Ariel University, Ariel 407000, Israel

Complete contact information is available at: <https://pubs.acs.org/10.1021/acs.jpcc.0c10384>

## Notes

The authors declare no competing financial interest.

## ACKNOWLEDGMENTS

The authors gratefully acknowledge the Russian Science Foundation (project 19-19-00076) for the financial support of this work.

## REFERENCES

- (1) Osborne, H. Symmetry as an aesthetic factor. *Comput. Math. Appl.* **1986**, *12*, 77–82.
- (2) Weyl, H. *Symmetry*; Princeton University Press, Princeton, 1989.
- (3) Wigner, E. P. *Symmetries and Reflections*; M.I.T. Press, Cambridge, 1970.
- (4) van Fraassen, B. C. *Laws and Symmetry*; Oxford University Press, Oxford, 1989.
- (5) Rosen, J. *Symmetry in Science: An Introduction to the General Theory*; Springer-Verlag, New York, 1995.
- (6) Elliott, J. P.; Dawber, P. G. *Symmetry in Physics*; Macmillan Press, London, 1979.
- (7) Lanczos, C. *The Variational Principles of Mechanics*, 4th ed.; Dover Publications, New York, 1986.
- (8) Wess, J.; Bagger, J. *Supersymmetry and Supergravity*; Princeton University Press, Princeton, 1983.
- (9) Hall, B. C. Quantum Theory for Mathematicians. In *Graduate Texts in Mathematics*; Springer, New York, 2013; Vol. 267.
- (10) Karassiov, V. P. Symmetry approach to reveal hidden coherent structures in quantum optics. General outlook and examples. *J. Russ. Laser Res.* **2000**, *21*, 370–410.
- (11) Chatterjee, S. K. *Crystallography and the World of Symmetry*; Springer Series in Materials Sciences; Springer, Berlin, 2008; Vol. 113.
- (12) El-Batanouny, M.; Wooten, F. *Symmetry and Condensed Matter Physics—A Computational Approach*; Cambridge University Press, Cambridge, 2010.
- (13) Bormashenko, E. Entropy, Information, and Symmetry: Ordered Is Symmetrical. *Entropy* **2020**, *22*, No. 11.
- (14) Bormashenko, E. Entropy, Information, and Symmetry; Ordered Is Symmetrical, II: System of Spins in the Magnetic Field. *Entropy* **2020**, *22*, No. 235.
- (15) Darvas, G. *Symmetry: Cultural-historical and Ontological Aspects of Science-Arts Relations*; Birkhauser, Basel, 2007.

- (16) Zabrodsky, H.; Peleg, S.; Avnir, D. Continuous symmetry measures. *J. Am. Chem. Soc.* **1992**, *114*, 7843–7851.
- (17) Zabrodsky, H.; Peleg, S.; Avnir, D. Continuous symmetry measures. 2. Symmetry groups and the tetrahedron. *J. Am. Chem. Soc.* **1993**, *115*, 8278–8289.
- (18) Zabrodsky, H.; Avnir, D. Continuous Symmetry Measures. 4. Chirality. *J. Am. Chem. Soc.* **1995**, *117*, 462–473.
- (19) Pinsky, M.; Avnir, D. Continuous Symmetry Measures. 5. The Classical Polyhedra. *Inorg. Chem.* **1998**, *37*, 5575–5582.
- (20) Zabrodsky, H.; Peleg, S.; Avnir, D. Symmetry as a continuous feature. *IEEE Trans. Pattern Anal. Mach. Intell.* **1995**, *17*, 1154–1166.
- (21) Fedorets, A. A. Droplet cluster. *J. Exp. Theor. Phys. Lett.* **2004**, *79*, 372–374.
- (22) Fedorets, A. A.; Dombrovsky, L. A.; Bormashenko, E.; Nosonovsky, M. On relative contribution of electrostatic and aerodynamic effects to dynamics of a levitating droplet cluster. *Int. J. Heat Mass Transfer* **2019**, *133*, 712–717.
- (23) Dombrovsky, L. A.; Fedorets, A. A.; Medvedev, D. N. The use of infrared irradiation to stabilize levitating clusters of water droplets. *Infrared Phys. Technol.* **2016**, *75*, 124–132.
- (24) Fedorets, A. A.; Bormashenko, E.; Dombrovsky, L. A.; Nosonovsky, M. Symmetry of small clusters of levitating water droplets. *Phys. Chem. Chem. Phys.* **2020**, *22*, 12239–12244.
- (25) Fedorets, A. A.; Frenkel, M.; Shulzinger, E.; Dombrovsky, L. A.; Bormashenko, E.; Nosonovsky, M. Self-assembled levitating clusters of water droplets: pattern-formation and stability. *Sci. Rep.* **2017**, *7*, No. 1888.
- (26) Barthélemy, M. Spatial networks. *Phys. Rep.* **2011**, *499*, 1–101.
- (27) Weaire, D.; Rivier, N. Soap, cells and statistics—random patterns in two dimensions. *Contemp. Phys.* **1984**, *25*, 59–99.
- (28) Arnold, V. I. *Symplectization, Complexification and Mathematical Trinities*; Fields Institute Commun., 1999; Vol. 24, pp 23–37.
- (29) Bormashenko, E.; Frenkel, M.; Vilks, A.; Legchenkova, I.; Fedorets, A. A.; Aktaev, N. E.; Dombrovsky, L. A.; Nosonovsky, M. Characterization of self-assembled 2D patterns with Voronoi entropy. *Entropy* **2018**, *20*, No. 956.
- (30) Ashcroft, N. W.; Mermin, N. D. *Solid State Physics*; Harcourt College Publishers, Fort Worth, 1976.
- (31) Brandmüller, J. An extension of the Neumann–Minnigerode–Curie principle. *Comput. Math. Appl.* **1986**, *12*, 97–100.
- (32) Fedorets, A. A.; Shcherbakov, D.; Dombrovsky, L. A.; Bormashenko, E.; Nosonovsky, M. Impact of surfactants on the formation and properties of droplet clusters. *Langmuir* **2020**, *36*, 11154–11160.
- (33) Lanczos, C. *The Variational Principles of Mechanics*; Dover Publications Inc., New York, 1986.
- (34) Casanova, D.; Llunell, M.; Alemany, P.; Alvarez, S. The rich stereochemistry of eight-vertex polyhedra: A continuous shape measures study. *Chem. - Eur. J.* **2005**, *11*, 1479–1494.
- (35) Zahrt, A. F.; Denmark, S. E. Evaluating continuous chirality measure as a 3D descriptor in chemoinformatics applied to asymmetric catalysis. *Tetrahedron* **2019**, *75*, 1841–1851.
- (36) Tuvi-Arad, I.; Alon, G. Improved algorithms for quantifying the near symmetry of proteins: complete side chains analysis. *J. Cheminf.* **2019**, *11*, No. 39.
- (37) Fedorets, A. A.; Aktaev, N. E.; Gabyshev, D. N.; Bormashenko, E.; Dombrovsky, L. A.; Nosonovsky, M. Oscillatory motion of a droplet cluster. *J. Phys. Chem. C* **2019**, *123*, 23572–23576.
- (38) Fedorets, A. A.; Bormashenko, E.; Dombrovsky, L. A.; Nosonovsky, M. Droplet clusters: nature-inspired biological reactors and aerosols. *Philos. Trans. R. Soc., A* **2019**, *377*, No. 20190121.
- (39) Dombrovsky, L. A.; Fedorets, A. A.; Levashov, V. Yu.; Kryukov, A. P.; Bormashenko, E.; Nosonovsky, M. Modeling Evaporation of Water Droplets as Applied to Survival of Airborne Viruses. *Atmosphere* **2020**, *11*, No. 965.